# UAV photogrammetry and 3D analyses of CH sites

## The millstone quarry district of Mayen (DE) as a case study

Stefanie WEFERS | Philipp ATORF | Jörg KLONOWSKI

i3mainz – Institute for Spatial Information and Surveying Technology, Mainz University of Applied Sciences

**Abstract:** Application and analysis capabilities of 3D data sets generated through UAV photogrammetry are presented on the basis of an exemplary millstone quarry of the so-called Mayen quarry district (Germany). In general, millstone quarries are technical cultural heritage sites which give evidence for economic interpretations as they are of interest for the reconstruction of ancient procurement patterns. Particularly those quarries which had a high economic impact cover large areas with often arduous accessibility. Therefore, photogrammetric recording using a UAV is the best approach for fast and inexpensive high-quality documentation.

The images are used to create a 3D data set and orthophoto. For analysis and interpretation the Spatial Image analysis and Visualisation Tool (SIVT) of i3mainz is used allowing a variety of interactive visualization functionalities. The 3D data are transformed into 2.5D data enabling segmentation of spatial information and volume calculations. Both functionalities support the cultural heritage expert's research: On the one hand the interactive segmentation allows producing a map of the quarry displaying only those parts associated with the extraction. On the other hand the output of the quarry including debris and millstone blanks can be calculated easily. All in all, the entire workflow beginning with data capture using a UAV followed by data processing, (2.5D / 3D) data analyses and visualisation of the results is presented.

**Keywords:** interactive data analyses, segmentation, volume calculation, cultural heritage documentation

### Introduction

Quern and millstone quarries of former periods are cultural heritage (CH) sites which give evidence for economic indicators such as production processes and output, while highlighting the organisation within the quarry (e.g. MANGARTZ 2008). When archaeological research addtionally encompasses studies of the products found outside of the quarry, the distribution area and channels can also be addressed (e.g. ANDERSON et al. 2003; WEFERS 2012). Generally, quarries with a high economic impact cover large areas, with quarrying marks and debris on different levels and on various scales. They are often difficult to access due to both high altitude differences and because of their remote locations, e.g. in mountainous areas (e.g. BAUG 2006; LONGEPIERRE 2006; PEACOCK 2013, 135-141). Therefore, a sound documentation and analysis of these CH sites with traditional methods such as mapping and documentation of quarry marks by photos and drawings is a challenge. We suggest using a VTOL-UAV (**V**ertical **T**ake-**O**ff and **L**anding – **U**nmanned **A**erial **V**ehicle) equipped with a camera and to use the photos to generate a digital 3-dimensional point cloud of the entire quarry area through photogrammetric methods and the Structure from Motion technique (e.g. NEITZEL and KLONOWSKI 2011). Besides a sound, detailed documentation and an

enhanced dissemination through online publishing possibilities, these data allow further processing steps supporting the research of CH experts.

For data analysis, we recommend the **S**patial **I**mage analysis and **V**iewing **T**ool (SIVT) which is a simple interactive tool tailored to the needs of CH experts, who are normally not familiar with conventional 3D analysis software.

> *"Apart from visualisation functionalities [this tool allows an] efficient interactive interpretation […] [by] a layer structure allowing superimposed display through transparency, mapping with multiple vector layers and metadata storage. This allows a holistic analysis of 3D-data and various 2D-data. Most appropriate are 3D-datasets representing objects with a flat surface containing features of interest which are either elevated from or recessed into the overall topography"*
>
> (WEFERS et al. in print).

However, also datasets such as the quarry data are appropriate.

A further functionality of SIVT on which we focus in this paper is the segmentation of relevant parts of the dataset. Applied to quarry data, this functionality supports the archaeological analysis efficiently as the output of a quarry, which is in our case the total numbers of produced millstones, can be easily quantified. This functionality was implemented based on the image segmentation method called watershed.

## State of the art

Up to now, quarries have been traditionally documented (including the mapping of the overall structure and detailed documentation of quarry marks and parcels) using photos and drawings as shown by several contributions in BELMONT and MANGARTZ (2006) as well as BUCHSENSCHUTZ et al. (2011). Besides our approach recording one of the quarry parcels in the Mayen quarry district using a VTOL-UAV, one of the first CH experts applying 3D techniques was Wolfgang CZYSZ (2015), who recorded a medieval quarry near Altenbeuern (Bavaria) with a Terrestrial Laser Scanner.

Since the occurrence of 3D datasets segmentation (of point clouds and meshes) has been part of research in fields of computer vision and geodesy/photogrammetry (DORNINGER and NOTHEGGER 2007; REITBERGER 2010) often related to applications of medical science, archaeology, or other disciplines (STAWIASKI et. al. 2008; RICHARDSON et al. 2013). There are many different approaches for segmentation. SHAMIR (2008) suggest a grouping into two main sections: part-type and surface-type segmentation. The aim of the former is to identify whole components of 3D objects, e.g. a 3D mesh of an airplane could be segmented into its body, wings, and fin (KALOGERAKIS et al. 2010). The latter approach tries to find a region on an object surface which shares similar properties. These properties are mostly geometric such as curvature or geodesic distance. Both categories can accomplish a variety of different techniques such as region growing (ZHANG et al. 2005) or graph cut (KATZ and TAL 2003).

As our aim is the segmentation of the surface of the quarry into relevant quarry areas we use its geometric information to identify the edges of these quarry extraction areas. RICHARDSON's et al. (2013) solution targets on an automatic generation of drawings for a specific group of CH objects (Neolithic chipped stone tools) having at the first glance similar characteristics as our case study: They intend to automatically find scars and ridges (significant for chipped stone tools) which would replace traditional documentation methods

of these tools, as well as to then classify these tools through their characteristics. The developed algorithm uses curvature and geodesic clustering for segmentation. It is customised for this specific application (chipped stone tools), performing quite accurately due to the fact that chipped stone tools in general share the same characteristics and the overall high number of chipped stone tools justifies such a development.
RICHARDSON et al. (2013) compare their results with a well-known “watershed” separation technique (VINCENT and SOILLE 1991) which has been first used for 3D meshes by MANGAN and WHITAKER (1998) and can also be used for 2D (2.5D DEM) images (BEUCHER and MEYER 1992). The results of this algorithm are not as accurate as their approach, but it is still able to find most of the stone tool’s ridges of interest. However, the main difference to our dataset is that the documentation of a chipped stone tool requires displaying almost all ridges, whereas in our case many edges and ridges are not of interest. Therefore, we used the well-known watershed separation technique.
Watershed transformation as described by BEUCHER and MEYER (1992) is an image segmentation technique interpreting intensity images as a topographic surface, where high intensity means high altitude. In special case, with simple and noise free data sets, it is able to generate a fully automated segmentation result. For very complex data, as in our case, semi-automatic segmentation including human interaction is the most promising approach (HAHN and PEITGEN 2003; STAWIASKI et. al. 2008).

## Mayen quarry and research question

Primarily young volcanic lava flows (from the Tertiary and Quaternary) have rock characteristics which are most suitable for querns and millstones used to produce flour or coarse meal from grain (WEFERS 2012, pp. 31-32). Quarries exploiting volcanic rock could especially achieve a high economic impact in the past (MANGARTZ 2008, 195-198). The quarry district around Mayen, Ettringen, and Kottenheim in the Eifel (Germany) is one of these cases, and was in use from Neolithic times until the 20$^{th}$ century (GLUHAK 2010, pp. 9-18). Its products were already distributed as far as to the British Isles in the North and to Austria in the South during the Roman era (GLUHAK and WEFERS 2011; PEACOCK 2013, pp. 151-154). In our study, we focus on one Late Iron Age to Early Roman Iron Age quarry covering an area of ca. 15 m x 15 m, with the bottom level varying between 278 and 280 m above sea level (fig. 1). It was excavated in 1999 and 2000, and is part of an archaeological park which is open to the public. The following workflow within a Roman quarry could be reconstructed through its excavation and studies of further extraction sites (fig. 2). The volcanic rock of the quarries of this region solidified in vertical columns of hexagonal or octagonal shape which is a typical geological structure of volcanic lava flows. These columns are the best precondition to produce rotary querns or millstones as they already provide the best shape to prepare circular millstones. First, a suitable column is selected and the workman marked a horizontal line on the column representing the sought breakage. This line served as orientation line for the preparation of either a notch or several wedge pockets having a width of ca. 5-12 cm (MANGARTZ 2008, pp. 275-276, No. 3-27 to 3-44 and Taf. 6, 7). Wedges were then inserted into the notch or wedge pockets, and the workman drove the wedges one after another deeper into the rock. Through this process, a block is extracted which is roughly shaped into a millstone blank within the quarry. After one block is extracted from a column, the same procedure starts for the next block. Through the extraction of blocks, adjacent columns are getting exposed which are also suitable for block extraction. This workflow

produces a quarry with cascaded bottom levels controlled by the columns. During the excavation, several dismissed millstone blanks were found (MANGARTZ 2008, pp. 107-121).

The information needed by the archaeologist can be identified through having this knowledge of the workflow within the quarry. The size, number of suitable columns, and the volume of the millstone blanks is relevant for the calculation of output and economic impact estimation. The different bottom levels and relics of notches and wedge pockets (having a size of only 5 to 10 cm) are also of interest for a better understanding of the workflow within the quarry.

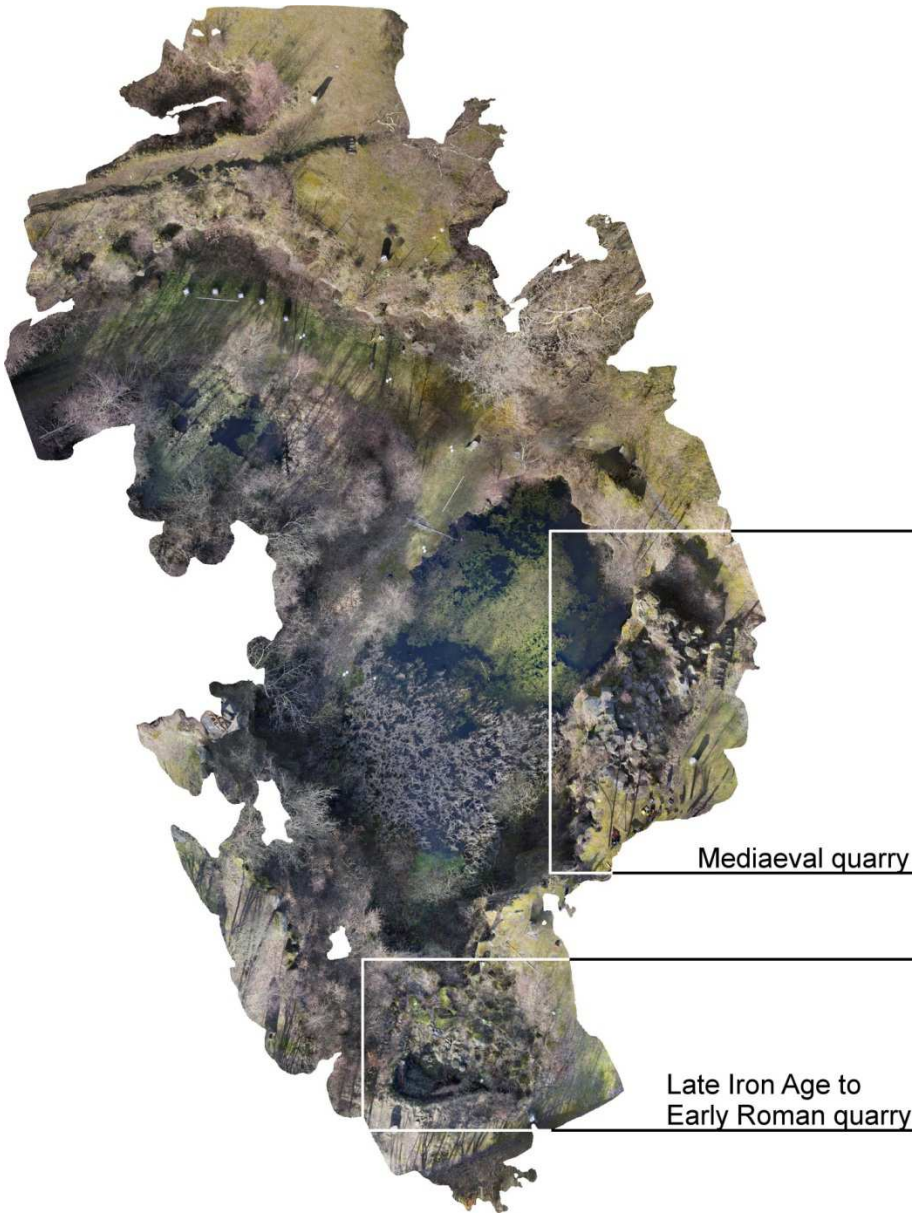


Fig. 1 – Orthophoto of the recorded quarry area in Mayen displaying the Late Iron Age to Early Roman quarry at the bottom, the Medieavel quarry on the right and the modern quarry in the middle and upper part. (i3mainz)

Fig. 2 – Illustration of quarrying processes in an idealised Roman millstone quarry of the Mayen quarry district. Background: columns of volcanic rock discarded for quarrying and used as boundary. Left: Piling up of debris behind dry stone walls. Middle: Production of millstone blanks. Right: Different exploitation steps to produce blanks from lava columns (copyright: design: A. Schmickler; MANGARTZ 2008, 115 fig. 39)

## 3D recording of the quarry

In order to generate a 3D documentation of the Mayen quarry district we decided to use UAV photogrammetry for data capture. Due to the limitation of space in and above the quarry by many obstacles such as big trees and bushes a VTOL-UAV, precisely an octocopter, was brought into use. The advantage of such a system is the enormous flexibility during the flight: the octocopter is capable of fully 3D flights as it can fly horizontal rows, vertical columns, or sloped tracks without the need for a minimum velocity (which is necessary using aeroplanes). Due to the number of obstacles within the quarry we used it remotely, although the copter is a multi-sensor platform with several sensors providing a predefined, autonomous flight (e.g. gyroscopes, accelerometers, an air pressure sensor, magnetic-compass GPS/GNSS). The photogrammetric survey was done with a **D**igital **S**ingle **L**ens **R**eflex (DSLR) camera *Canon EOS 5D Mark III* (5760 x 3840 pixel, CMOS-CHIP 36 x 24 mm) and a wide-angle lens with 24 mm focal length. The duration of one flight is mainly limited by the capacity of the battery packs (Lithium-Polymer). We used 5 packs, every pack lasts ca. 5-8 minutes. The 5 flights were used for different test scenarios using an automated trigger for the camera (every 3, 5 or 8 seconds) as well as manually triggering the camera. In every scenario the goal to get an image overlap of at least 60 % was realised. The flight height was 15-20 m. Thus, the photogrammetric survey led to 323 digital photos, each ca.15-20 MB.

In order to be able to achieve georeferenced and scaled results 17 target plates were placed well distributed in the quarry area (horizontal and vertical) before the photogrammetric survey. Using the Satellite Positioning

Service *SAPOS*® we determined the GNSS coordinates of the targets and transformed them into the Gauss-Krueger coordinate system. The SAPOS® Service “HEPS”, which is a real time kinematic GNSS measurement, leads to an accuracy of the transformed coordinates of ca. 2 cm.

## Data processing

The data processing is done with the SfM-Tool (**S**tructure **f**rom **M**otion) PhotoScan (developing company AgiSoft, Russia). SfM is able to automatically generate 3D point clouds from arbitrary (highly overlapping) image configurations. For the computation of point clouds Exif metadata (stored in the header of every digital image) provides information on image size and applied focal length of the camera.

First, PhotoScan automatically extracts features such as feature points, edges, and contours which are stable under lightning and viewpoint variations and generates a descriptor for each point regarding its local neighbourhood. These descriptors are used during the computation process detecting correspondences across the photos in order to describe homologous areas. This SIFT approach (**S**cale **I**nvariant **F**eature **T**ransform) for feature point detection was introduced by LOWE (2004).

Second, an algorithm computes interior and exterior orientation of the camera and refines the results iteratively by using bundle adjustments (greedy algorithm). During the adjustment calibration parameters of the camera are estimated.

Third, dense 3D point clouds are derived as a surface reconstruction from rectified and oriented images either by multi-view stereo approaches (FURUKAWA et al. 2010) or based on pair-wise depth map computation in overlapping areas of adjacent images (FURUKAWA and PONCE 2010).

Finally, PhotoScan computes the texture mapping by triangulation and parametrisation of the surface cutting it into smaller pieces and blending the source photos to form a texture atlas.

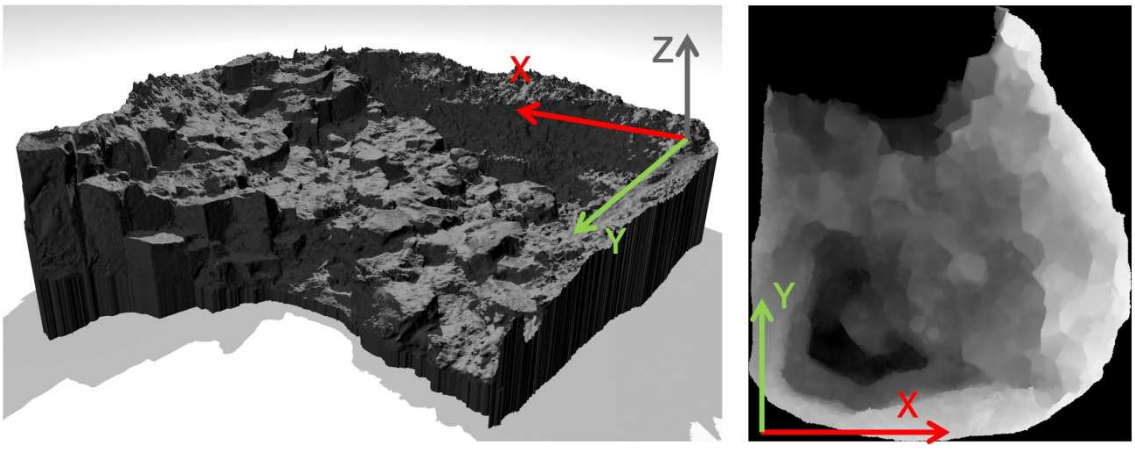


Fig. 3 – Block diagram of the 3D data set (left) and the related DEM deduced from the 3D data (right) of the Late Iron Age to Early Roman millstone quarry. Z-values of the 3D data are displayed as grey values for each pixel of the DEM (dark = deep areas; bright = high areas). (Copyright: i3mainz)

The results are a 3D point cloud coloured by the source photos and a textured mesh (model). Via GNSS control points the results are georeferenced and scaled. The computation time of the dense point cloud on the basis of 323 images took 22 hours; additional 2 hours were needed to create a textured mesh.

Although the total size of the recorded area has a size of 2,000 m², the Late Iron Age-Early Roman quarry has a size of only 400 m². The data are exported from PhotoScan as a DEM (Digital Elevation Model, understood as a 2.5D representation of a surface) (fig. 3) and an orthophoto (fig. 4) for further analysis and viewing. The 3D points are projected onto a plane that is normally vertical to the z-axis of the coordinate frame and is located above the surface in order to generate the DEM. This plane is divided into pixels of a given size. For every pixel, the nearest surface point is projected parallel onto the plane and the pixel gets the z-axis-value (elevation) of this surface point. Through this process, an image is generated in which each pixel includes the surface elevaton information.

Fig. 4 – Orthophoto of the Late Iron Age to Early Roman millstone quarry. (Copyright: i3mainz)

The orthophoto is similar to the DEM in terms of projecting the surface onto a plane. The difference is that the pixel includes the colour information of the surface, and not the elevation information.

By reducing the 3D data to 2.5D, some of the information such as the vertical object information gets lost. However, this is neglectable in the case of the Mayen quarry, as the main information can be examined by looking at height differences. Also, the Mayen quarry has no occluding areas such as caves or overhangs, which would not be captured in a 2.5D DEM.

### Data analysis – Segmentation functionality

As mentioned above, RICHARDSON et al. (2013) detect geometric ridges to automatically generate 2D drawings. This is also the case for the quarry data. There are some similarities between their and our raw data. Both surfaces are divided by geometric edge with the aim of finding areas which are enclosed by these edges. The main difference is that in our case (a typical quarry data set), the variance of the edges is very high. Some edges divide two column heads by a height difference of only a few centimeters, and others by a few decimeters. Additionally, the surface of each column head is not as flat and homogenous as surfaces of chipped stone tools, which have concave scars divided by distinct ridges. The results achieved by the approach described by RICHARDSON et al. (2013) would need an interactive revision of the generated lines. To reduce complexity, the 3D data of the Mayen quarry can be reduced to 2.5D data. This also helps with data sharing and interoperability because of smaller data sizes and use of known image data formats (JPEG, TIFF, and PDF). In addition, traditional excavation maps are 2D and are commonly understood by archaeologists. Based on these factors, we decided against RICHARDSON's et al. (2013) approach and to use a marker based watershed approach for segmentation. In this method, an intensity image is interpreted as mountains and valleys of a surface, where high intensity infers mountains and low intensity describes valleys. The idea of the watershed is to define regions that belong to one valley (BEUCHER and MEYER 1992). This is done by digitally flooding valleys with a weighted effect that acts similar to water, with every local minimum sequentially becoming a catchment basin. As the "water level" rises, two adjacent basins share one border line at a specific height, the so-called watershed. Most images have many local minima leading to a very extensive segmentation through the watershed functionality, leading to over-segmentation. To be able to control the segmentation process, a modified watershed transformation exists called the marker-controlled watershed transformation (BEUCHER and MEYER 1992). It enables the definition of markers (regions) before using the watershed functionality. These markers define from where the water should start rising. This allows water to flow into adjacent valleys which do not belong to a marker region. Only if two marker regions touch each other is a watershed defined. The result is a less extensive segmentation. However, the definition of the marker regions is to be decided for each individual dataset. In our approach we use first an automatic generation of these markers to create adequate preliminary results which are further on interactively treated by the CH expert.

As described above our segmentation method is based on a marker-controlled watershed using the OpenCV Library (BRADSKI 2000). The source image for our approach is a DEM generated from the 3D mesh. As the available mesh is georeferenced, the DEM is created using *Agissoft Photoscan*. The needed configuration parameters are a projection plane, defined by the x- and y-axis of the coordinate system (in our case Gauss-Krueger), and the pixel size which defines the ground resolution of the DEM. Besides a raw image, the OpenCV implementation expects a second input, which defines the marker regions and has to be computed in

advance. These markers can represent both regions where there should be no edge and regions where the watershed algorithm should find an edge.

The definition of the markers of the Mayen quarry consists of three steps. As most of the columns in the Mayen quarry are distinguished through a height difference, we first have to find these edges in the DEM. This is done by the canny edge detector which asks for the following steps: First, to reduce noise, a Gaussian filter is applied to the original image. Second, the gradients strength and orientation are calculated. Third, a non-maximum suppression is used generating edges which have a width of one pixel. Fourth, two thresholds (upper and lower) are applied to the image. If a pixel's gradient value is higher than the upper threshold it is marked as an edge. If a pixel's gradient value is lower than the lower threshold it does not belong to an edge. If a pixel's gradient value is between the lower and upper threshold and a neighbouring pixel is marked as an edge than the pixel is also part of an edge (CANNY 1986). These thresholds have to be set in advance. The thresholds have to be set individually and depend on the aim of the segmentation and content of the image. Generally, the thresholds define how many edges are found in the image, leading to an over- or under-segmentation of the source image in the case of inadequate threshold settings (fig. 5).

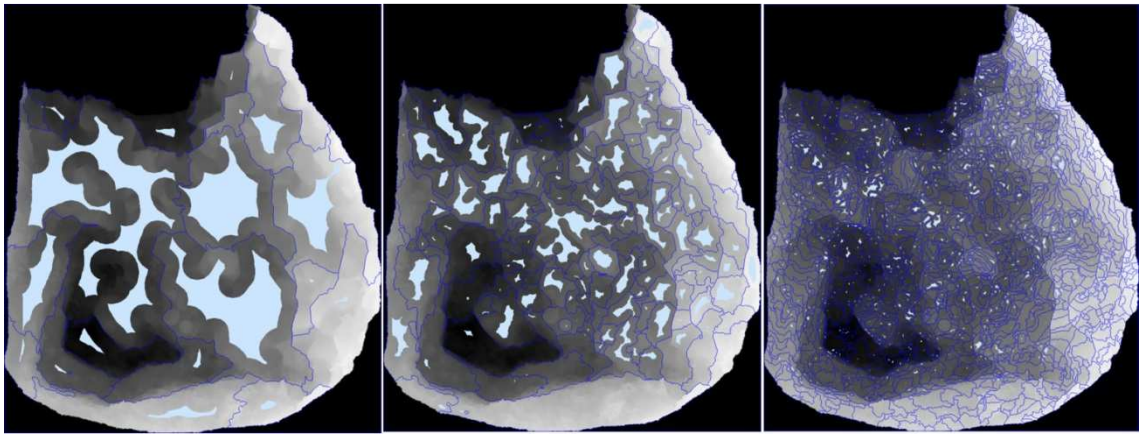

Fig. 5 – Result of the marker based watershed with different canny parameters. The light-blue areas display the generated seed region from where the "water level" rises. Dark-blue lines are the generated watersheds. Left: under segmentation due to a low canny parameter (30 and 60). Middle: best pre-segmentation due to canny thresholds 12 and 24. Right: canny thresholds 2 and 4 lead to an over-segmentation. (Copyright: i3mainz)

The second step of the marker definition is a distance transformation, followed by the third step, which is thresholding the result (fig. 6). Our approach to these two steps is similar to the one by BEUCHER and MEYER (1992) in terms of using a distance function to divide overlapping regions. The distance transformation calculates the distance of every pixel to its nearest edge. The result can be interpreted as a surface where valleys are the edges and the height of the mountains reflects the distance to the valley (edge). The markers we would like to create have to consist of coherent regions. To achieve this, the distance transformation result is grouped. By thresholding the result, the image is divided into two parts: mountains and valleys. Mountains represent areas where there should be no edge and valleys are areas where the watershed algorithm should find the edges. A final operation must additionally be performed to generate markers which leave a unique value for every region. This is done by connected component labelling, an

image processing technique that groups connecting pixels which share the same value (OpenCV implementation based on WU et. al 2008). The result is used as a basis for the further steps.

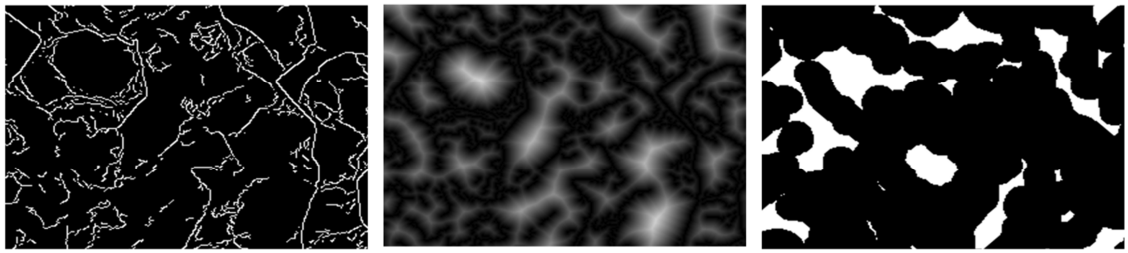

Fig. 6 – Pre-processing steps to create the marker regions. Left: result of the Canny edge detector. Middle: distance transformation of the previous step. The brighter the region the higher the distance to an edge. (right) marker regions (white) and non-marker regions (black) after thresholding the distance transformation result.

Now the watershed algorithm can be applied to the quarry DEM and the marker layer. The result largely depends on the thresholds of the Canny operator. To avoid over- or under-segmentation, the best thresholds for the gradient values for the Mayen data set are 12 (lower) and 24 (upper). These parameters depend on the dataset and must be adapted individually. The result of the watershed transformation is an approximated segmentation of the quarry still including incorrect areas (fig. 5). The preliminary result needs further interactive processing.

The interactive processing of the automatic segmentation results focusses on the usability since the tool will be used by CH experts with low technical competence. Our tool, like STAWIASKI et al. 2008, deals with this by changing the markers. This is done by painting on this layer with a brush (left mouse button) or eraser (right mouse button) allowing for automatic removal of created watersheds (segmentation boundaries) or the creation of new catchment basins which are the seed of a new segmentation region (fig. 7). The watershed transformation is repeated with the manipulated marker layer allowing to interactively optimise the result (see below).

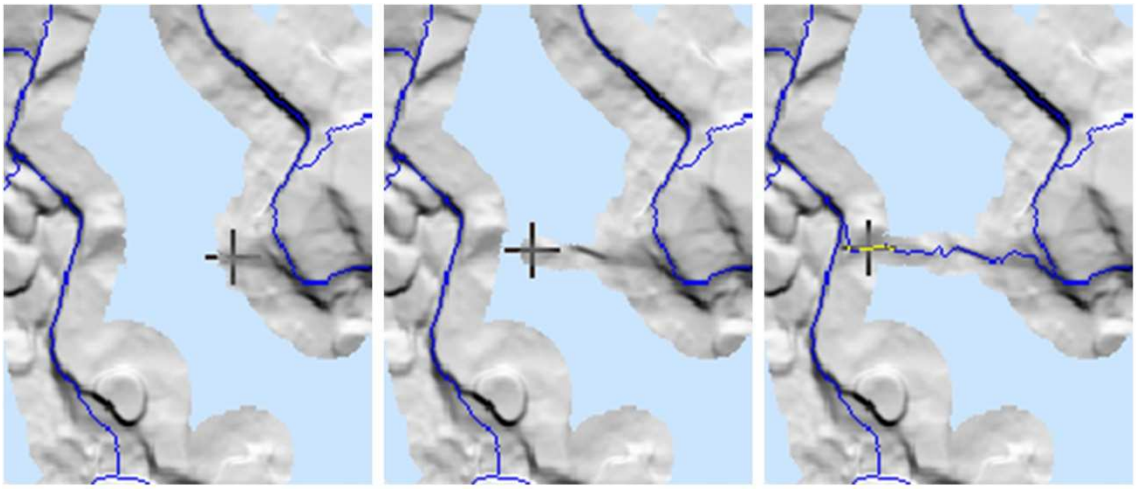

Fig. 7 – Interactive editing of the automatically predefined markers (light-blue) generating a new watershed (dark-blue). (Copyright: i3mainz)

**Volume calculations**

Volumetric information of the quarry is needed to determine the quarry output. As the quarry is not a closed body, which would be necessary for a volume calculation, the quarry is covered by a virtual top cover. The calculation cannot be done using PhotoScan because it needs a solid closed mesh. However, we can use the already created DEM for volume calculations. The calculation consists of two steps: First the user has to define an elevation. This elevation serves as top cover of the quarry and the calculation returns the volume between the quarry surface and this cover. Next the elevation difference from the surface to this lid is calculated for every pixel. This is done by subtracting the previously defined elevation of the DEM values for each pixel. This means a pillar from the quarry surface to the cover is defined for every pixel. The sums of all these pillars form the quarry volume. The volume can be calculated metrically through knowledge of the pixel size. This method assumes that the original surface of the quarry was planar, which is suitable for our case study (fig. 8).

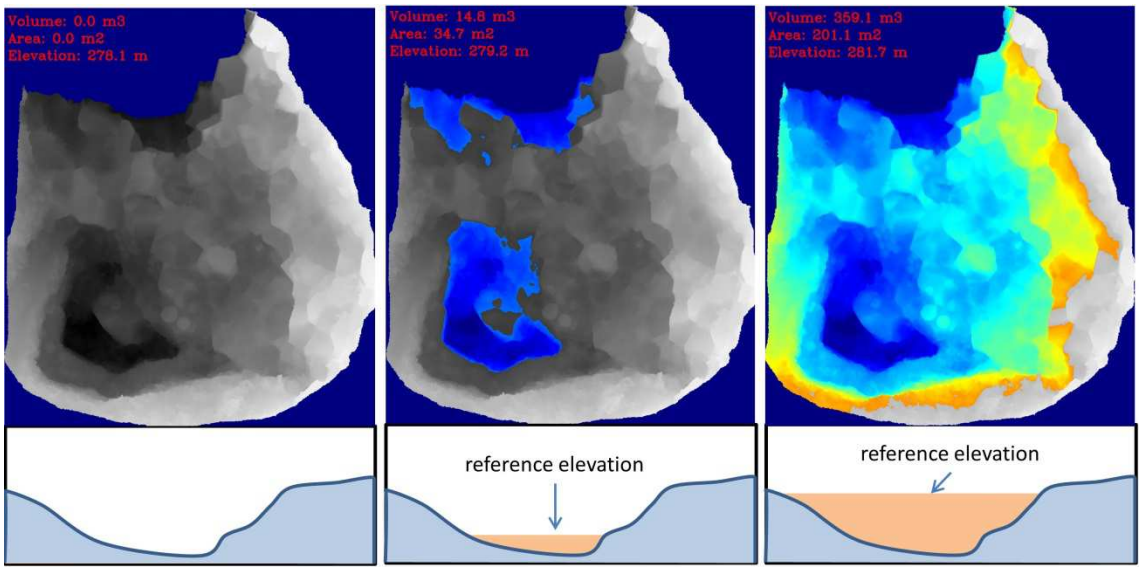


Fig. 8 – Volume calculation with water filling functionality. By increasing the reference elevation the water filling functionality illustrates the maximum elevation and the volume underneath it. (Copyright: i3mainz)

One aim of the analysis-tool is that it should be user-friendly, which means reducing the complexities of all interaction steps. The user has to choose a target elevation for the volume calculation. By changing the elevation, the user gets a direct feedback through the water-filling functionality applied to the DEM (WEFERS et al. in print). Thus, the user sees exactly which parts are underneath the “top cover” and can adjust the elevation as needed.

One advantage is that the segmentation result can be used to calculate the volume of one single volcanic column. This is useful to analyse only parts of the quarry.

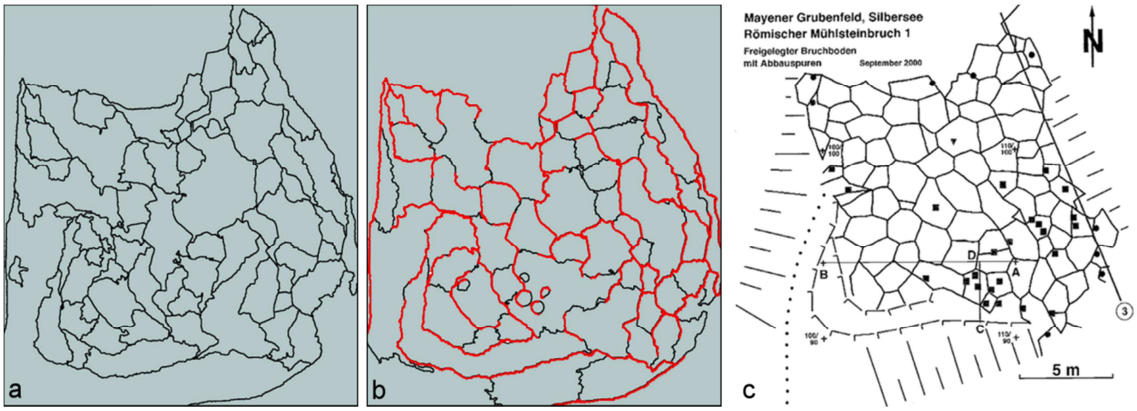


Fig. 9 – Comparison of automatic and interactive segmentation results with the excavation map: a: automatic segmentation result. – b: result after interactive revision with red lines representing those lines which were already automatically generated. – Right: excavation map which is used as ground truth. (Copyright: a and b: i3mainz; c: Mangartz 2008, 110 fig. 36)

## Discussion

Fig. 9a displays the result of the automatic segmentation functionality applied to the DEM of the Late Iron Age to Early Roman quarry. The excavation map (fig. 9c) produced during the excavations in 1999 and 2000 is used as a ground truth. Through manual post-processing which lasted about half an hour the automatically produced map was adjusted always using the excavation map as ground truth. Fig. 9b displays the result after manual post-processing. The red lines represent those lines which were already automatically generated, whereas the black lines represent those which were added or changed through the post-processing. The other way around, comparing the result of the automatic segmentation with the result of the post-processing illustrates how many lines (displayed in black) had to be removed (fig. 10).

Projecting the manually processed segmentation map onto the excavation map (fig. 11) illustrates the overall good result of the segmentation approach. Especially in the areas highlighted in green it was possible to reproduce the excavation map. However, in the grey highlighted areas it was only possible to generate segmentation lines encompassing more than one column head. This is due to the fact that those columns outlined by the segmentation line have the same height. This clearly illustrates that the excavation map not only displays height or geometric differences but also cracks in-between columns of the same height. Therefore, other functionalities need to be applied to be able to generate such segmentation lines.

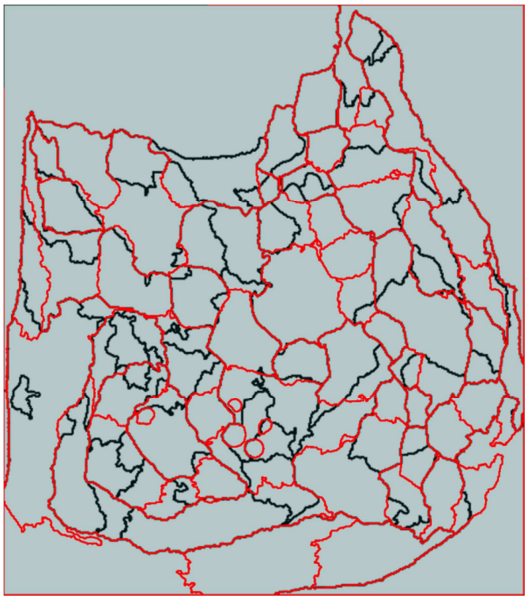

Fig. 10 – Comparison of the automatic segmentation result with the segmentation result after manual post-processing. The black lines represent those lines which had to be removed manually. (Copyright: i3mainz)

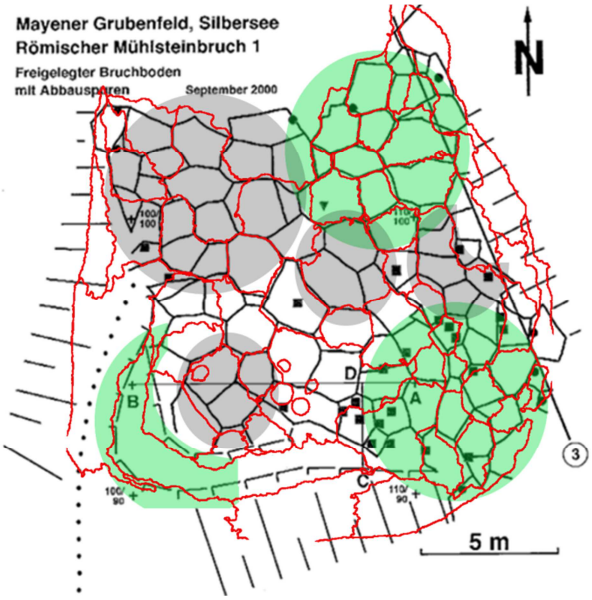


Fig. 11 – Comparison of the segmentation result after manual post-processing with the excavation map. Green – reproduction of the excavation map. Gray – segmentation lines encompass more than one column head. (Copyright: i3mainz)

The millstone blanks found during excavation have radii between 18 cm and 31 cm. Two major groups could be defined, the first one with radii between 19 cm and 20 cm and the second one with radii between 21.5 cm and 23 cm. As the larger examples (radius above 25 cm) all show only a rough condition of preparation, it is assumed that the major part of the millstones should have radii between 18 cm and 20 cm. The thickness of the millstones varied between 10 cm and 15 cm, and a radius to thickness ratio between 1.5:1 and 2:1 is assumed (MANGARTZ 2008, pp. 118-120).

Volumes of the millstone blanks vary between 10.000 and 30.000 $cm^3$:

Volume $V = \pi r^2 h$

r = 25 cm; h = 15 cm: $V = \pi\ 25^2\ 15 = 29{,}452\ cm^3$

r = 23 cm; h = 15 cm: $V = \pi\ 23^2\ 15 = 24{,}929\ cm^3$

r = 21 cm; h = 13 cm: $V = \pi\ 21^2\ 13 = 18{,}011\ cm^3$

r = 20 cm; h = 15 cm: $V = \pi\ 20^2\ 15 = 18{,}850\ cm^3$

r = 18 cm; h = 10 cm: $V = \pi\ 18^2\ 10 = 10{,}179\ cm^3$

The average volume of the millstones produced in the quarry is assumed to be 20,000 $cm^3$ as the better part of the blanks at hand have radii between 18 cm and 20 cm. As almost all columns are suitable for quarrying – roughly 62 columns – the volume calculation was applied to the entire quarry represented by the DEM. The area of each column head was used to determine if the pillar would be suitable for quarrying, using the requirement that a circle of at least a 36 diameter could fit internally. The volume calculation functionality shows that the entire volume of the quarry is 360 $m^3$ (fig. 8), which means that this amount of volcanic rock was removed from the quarry in Late Iron Age/Early Roman times. If the entire volume of the quarry could have been used to produce millstone blanks without any debris and space in-between the products, 18,000 blanks could have been produced. However, due to the high amount of debris produced during quarrying and

blank production, as well as discarded blanks due to natural cracks within the rock, this number has to be reduced. Generally, it is assumed that five complete rotary querns, consisting of a lower and an upper stone, were produced per 1 cubic meter (MANGARTZ 2008, p. 124). Therefore, it is assumed that roughly 3,600 blanks could have been produced by Roman workmen just in this single quarry over a period of many years. At first glance this seems to be a production output which is too high. However, MANGARTZ (2008, pp. 93-97) has assumed production rates of ca. 30,000 querns and millstones per year out of the entire Mayen quarry district. All in all, if the number of Roman quarry parcels would be known, MANGARTZ's (2008, pp. 93-97) assumption could be reassessed easily. Our calculations for a single quarry parcel could be extrapolated, especially considering that Roman quarry parcels had almost all of the same dimensions (MANGARTZ 2008, pp. 90-93).

## Conclusion

Altogether, the documentation of a quarry through photogrammetric recording strategies using a VTOL-UAV is fast and inexpensive. The processing of the unsorted overlapping photos with the SfM algorithm leads directly to several useful results: e.g. a coloured, georeferenced, and scaled 3D point cloud, a textured mesh (model), a DEM, and an orthophoto. While the amount of data in a point cloud is large the DEM and ortophoto support data sharing and interoperability because of smaller data sizes. In addition, the used data formats (JPEG, TIFF, and PDF) are well-known worldwide. All in all, an ideal basis supporting interdisciplinary discussions between CH experts all over the world is given. The need for the CH experts to work at the archaeological site is reduced. The visualisation and data handling using SIVT is recommended for CH experts because the archaeological analysis is enhanced through different functionalities such as the automatic and interactive image segmentation. Columns suitable for quern production can be detected and an output calculation is easily possible. However, the goal to produce a 2D visualisation of the quarry which is close to the excavation map needs additional functionalities complementing the interactive segmentation functionality.

First, this is due to the fact that from a technical point of view, an excavation map displays a variety of different and not only geometric information. However, the presented results could be improved through a combined visualisation of e.g. an orthophoto and the DEM within SIVT. This would support the detection of cracks and columns without height differences through the colour information of the orthophoto.

Second, using the recorded data of the Mayen quarry the detection of wedge pockets and notches is not possible due to the small size of these traces of quarrying and the ground resolution per pixel of 0.5 centimeter. However, in general a small size of an object of interest is no problem. This is due to the fact that a VTOL-UAV can be used with high flexibility, e.g.a lower flight height leads to a higher ground resolution. Thus, the copter serves as a kind of inspection tool to reach every point of interest of the quarry subject to the needs of the CH expert. As the SIFTalgorithm (scale invariant) is used, the photos taken from different heights (scales) could be commonly processed.

All in all, through a photogrammetric recording of a quarry a variety of different data sets can be generated. On the one hand these data sets support the archaeological research through different visualization and analysis possibilities as well as different options for data sharing. On the other hand the data sets can be used for dissemination purposes and archiving.

## Acknowledgements

We would like to acknowledge the support of Dipl.-Ing. (FH) Christian Sell and Dipl.-Ing. Willi Sell (both Ingenieur- und Vermessungsbüro Sell and CopterCam AG) who performed the UAV flight with their equipment. Furthermore, we would like to thank Dr. Holger Schaaff (Kompetenzbereich Vulkanologie, Archäologie und Technikgeschichte of the Römisch-Germanisches Zentralmuseum – Leibniz Forschungsinstitut für Archäologie) who organized the permission for data acquisition in Mayen.

## References

ANDERSON, T.J., AGUSTONI, C., DUVAUCHELLE, A., SERNEELS, V. and CASTELLA, D. (2003) *Des Artisans à la Campagne. Carrière de meules, forge et voie gallo-romaines à Châbles (FR)*. Archéologie Fribourgeoise 19. Fribourge: Academic Press.

BAUG, I. (2006) The quarries at Hyllestad – Production of quern stones and millstones in Western Norway. In: BELMONT, A. and MANGARTZ, F. eds. (2006) pp. 55-59.

BELMONT, A. and MANGARTZ, F. eds (2006) *Millstone quarries. Research, protection and valorization of an European Industrial Heritage (Antiquity-21th century). International Colloque Grenoble – 22th-25th of September 2005 – Maison des Sciences de l'Homme-Alpes*. Mainz: Verlag des Römisch-Germanischen Zentralmuseums.

BUCHSENSCHUTZ, O., JACCOTTEY, L., JODRY, F. and BLANCHARD, J.-L. eds (2011) *Évolution typologique et technique des meules du Néolithique à l'an mille. Actes des 3e Rencontres Archéologiques de l'Archéosite gaulois*. Aquitania Supplément 23. Bordeaux: Fédération Aquitania.

BEUCHER, S. and MEYER, F. (1992) The morphological approach to segmentation: the watershed transformation: mathematical morphology in image processing. *Opt. Eng.*, 34, pp. 433–481.

BRADSKI, G. (2000) OpenCV. *Dr. Dobb's Journal of Software Tools*, 2000.

CANNY, J. (1986) A computational approach to edge detection. *IEEE Transactions on Pattern Analysis and Machine Intelligence (PAMI)*, 6, pp. 679-698.

CZYSZ, W. (2015) Mühlsteinhauer im bayerischen Inntal. In: MAŘÍKOVÁ, M. and ZSCHIESCHANG, C. eds. *Wassermühlen und Wassernutzung im mittelalterlichen Ostmitteleuropa*. Forschungen zur Geschichte und Kultur des östlichen Mitteleuropa, Bd. 50. Stuttgart: Franz Steiner Verlag. pp. 279-308.

DORNINGER, P. and NOTHEGGER, C. (2007) 3D segmentation of unstructured point clouds for building modelling. *International Archives of the Photogrammetry, Remote Sensing and Spatial Information Sciences*, 35(3/W49A), pp. 191-196.

FURUKAWA, Y., CURLESS, B., SEITZ, S.M. and SZELISKI, R. (2010) Towards Internet-scale multi-view stereo. *IEEE Conference on Computer Vision and Pattern Recognition (CVPR)*, pp. 1434-1441.

FURUKAWA, Y. and PONCE, J. (2010) Accurate, Dense, and Robust Multiview Stereopsis. *IEEE Transactions on Pattern Analysis and Machine Intelligence (PAMI)*, 32(8), pp. 1362-1376.

GLUHAK, T.M. (2010) *Petrologisch-geochemische Charakterisierung quartärer Laven der Eifel als Grundlage zur archäometrischen Herkunftsbestimmung römischer Mühlsteine*. PhD thesis. Johannes Gutenberg-Universität Mainz.

GLUHAK, T.M. and WEFERS, S. (2011) Geochemische Herkunftsbestimmung römischer Getreidemühlen vom Magdalensberg, Kärnten. In: J. CEMPER-KIESSLICH ed. *Secundus conventus austriacus archaeometriae: Tagungsband zum Zweiten Österreichischen Archäometriekongress, 13. - 14. Mai 2010*. Salzburg: Eigenverl. Univ. Salzburg. pp. 79-82.

HAHN, H. K. and PEITGEN, H. O. (2003) IWT-interactive watershed transform: a hierarchical method for efficient interactive and automated segmentation of multidimensional gray-scale images. *Medical Imaging 2003: Image Processing,* 5032, pp. 643-653.

KALOGERAKIS, E., HERTZMANN, A. and SINGH, K. (2010*)* Learning 3D mesh segmentation and labeling. *ACM Transactions on Graphics (TOG)*, 29(4), p.102.

KATZ, S. and TAL, A. (2003) Hierarchical mesh decomposition using fuzzy clustering and cuts. *ACM Transactions on Graphics (TOG) – Proceedings of ACM SIGGRAPH 2003*, pp. 954-961.

LONGEPIERRE, S. (2006) Aux environs de Saint-Quentin-La-Poterie (Gard) durant l'Antiquité tardive: une microrégion très impliquée dans l'activité meulière. In: BELMONT, A. and MANGARTZ, F. eds. *Millstone quarries. Research, protection and valorization of an European Industrial Heritage (Antiquity-21th century). International Colloque Grenoble – 22th-25th of September 2005 – Maison des Sciences de l'Homme-Alpes*. Mainz: Verlag des Römisch-Germanischen Zentralmuseums. pp. 47-54.

LOWE, D. (2004) Distinctive image features from scale invariant keypoints. *International Journal of Computer Vision*, 60(2), pp. 91-110.

MANGAN, A. P. and WHITAKER, R. T. (1998) Surface segmentation using morphological watersheds. I*EEE Visualization 1998 Late Breaking Hot Topics*.

MANGARTZ, F. (2008) *Römischer Basaltlava-Abbau zwischen Eifel und Rhein*. Monographien RGZM 75. Vulkanpark-Forschungen 7. Mainz: Verlag des Römisch-Germanischen Zentralmuseums.

NEITZEL; F. and KLONOWSKI, J. (2011) Mobile 3D Mapping with a low-cost UAV System. *International Archives of the Photogrammetry, Remote Sensing and Spatial Information Sciences*, 38(1/C22), UAVg-2011, Conference on Unmanned Aerial Vehicle in Geomatics, Zurich, Switzerland.

PEACOCK, D. (2013) *The stone of life. Querns, mills and flour production in Europe up to c. AD 500*. Southampton Monographs in Archaeology New Series 1. Exeter: The Short Run Press Ltd.

REITBERGER, J. (2010) *3D-Segmentierung von Einzelbäumen und Baumartenklassifikation aus Daten flugzeuggetragener Full Waveform Laserscanner*. Dissertation, Deutsche Geodätische Kommission, Reihe C, Heft 652, München.

RICHARDSON, E., GROSMAN, L., SMILANSKY, U. and WERMAN, M. (2013) Extracting scar and ridge features from 3D-scanned lithic artifacts. In: EARL, G., SLY, T., CHRYSANTHI, A., MURRIETA-FLORES, P., PAPADOPOULOS, C., ROMANOWSKA, I. and WHEATLEY D. eds. *Archaeology in the Digital Era. Papers from the 40th Annual Conference of Computer Applications and Quantitative Methods in Archaeology (CAA), Southampton, 26-29 March 2012*. Amsterdam: Amsterdam University Press. pp. 83-92.

SHAMIR, A. (2008) A survey on mesh segmentation techniques. *Computer graphics forum*, 27(6), pp. 1539-1556.

STAWIASKI, J., DECENCIÈRE, E. and BIDAULT, F. (2008) *Interactive liver tumor segmentation using graph cuts and watershed*. In: Workshop on 3D Segmentation in the Clinic: A Grand Challenge II. Liver Tumor Segmentation Challenge. MICCAI.

VINCENT, F. and SOILLE, P. (1991) Watersheds in digital Spaces: An Efficient Algorithm Based on Immersion Simulations. *IEEE Transactions of Pattern Analyses and Machine Intelligence (PAMI)*, 13(6), pp. 583-598.

WEFERS, S. (2012) *Latènezeitliche Mühlen aus dem Gebiet zwischen den Steinbruchrevieren Mayen und Lovosice*. Monographien RGZM 95. Vulkanpark-Forschungen 9. Mainz: Verlag des Römisch-Germanischen Zentralmuseums.

WEFERS, S., REICH, T., TIETZ, B. and BOOCHS, F. (in print) SIVT – Processing, viewing and analysis of 3D scans of the porthole slab and slab b2 of Züschen I. In: *Proceedings of CAA 2015 – Keep the Revolution Going. 43rd Computer Applications and Quantitative Methods in Archaeology Annual Conference, University of Siena, 30 March-3 April 2015*.

WU, K., OTOO, E. and SUZUKI, K. (2008) *Two strategies to speed up connected component labeling algorithms*. LBNL Tech Report LBNL-59102.

ZHANG, E., MISCHAIKOW, K. and TURK, G. (2005) Feature-based surface parameterization and texture mapping. *ACM Transactions on Graphics (TOG)*, pp. 1-27.

**Imprint:**

Proceedings of the 20th International Conference on Cultural Heritage and New Technologies 2015 (CHNT 20, 2015)

Vienna 2016

http://www.chnt.at/proceedings-chnt-20/

ISBN 978-3-200-04698-6

Editor/Publisher**:** Museen der Stadt Wien – Stadtarchäologie

Editorial Team: Wolfgang Börner, Susanne Uhlirz